

Nikhef 2013-037

An extended Heitler-Matthews model for the full hadronic cascade in cosmic air showers.

J.M.C. Montanus

Nikhef

December 10, 2013

Abstract

The Heitler-Matthews model for hadronic air showers will be extended to all the generations of electromagnetic subshowers in the hadronic cascade. The relation between interaction length and the thickness of the cascade layers is revisited. The analysis is outlined in detail for showers initiated by primary protons. For showers initiated by iron primaries the part of the analysis is given for as far as it differs from the analysis for a primary proton. Predictions for shower sizes and the depth of maximum shower size are compared with results Monte Carlo simulations. As for the Heitler-Matthews model the present model predicts too small values for the depth of maximum shower size. The application of the Heitler-Matthews model to the first generation of electromagnetic subshowers leads to an overestimation of the elongation rate. The application of the Heitler-Matthews model to all the generations of electromagnetic subshowers results in an elongation rate which decreases for increasing energy. The discrepancy with respect to predictions from Monte Carlo models can therefore not be explained by disregarding the second and higher generations in the hadronic cascade. An alternative explanation will be proposed.

1 Introduction

A simplified description of the longitudinal evolution of electromagnetic showers is given by the Heitler model [1]. Starting with a primary particle of energy E_0 , the number of particles doubles every splitting length $d = \lambda_r \ln 2$, where the radiation length λ_r is about 37 g cm^{-2} . The doubling stops when the energy per particle is equal to the critical energy $\xi_c^e \approx 85 \text{ MeV}$. The resulting Heitler profile is

$$N(X) = \begin{cases} 2^{X/d} & , X \leq n_c^e d ; \\ 0 & , X > n_c^e d , \end{cases} \quad (1)$$

where n_c^e is maximum the number of steps: $n_c^e \ln 2 = \ln(E_0/\xi_c^e)$.

A Heitler model for the hadronic cascade in air showers has been constructed by Matthews [2]. The Heitler-Matthews model is useful for the explanation of hadronic cascades as well as for the analytical derivation of relations between quantities as primary energy, muon number, electron number and depth of maximum shower size [3, 4, 5]. For the prediction of the number of charged particles it is assumed that each hadronic interaction results in $M_{\text{ch}} = 10$ charged pions and $\frac{1}{2}M_{\text{ch}} = 5$ neutral pions. That is, the total multiplicity M is equal to 15. The neutral pions initiate electromagnetic subshowers when they decay into photons. For the prediction for the depth of maximum shower size, restricted to the first generation of electromagnetic subshowers, the multiplicity and interaction length are parameterized by the energy of the interaction.

The atmosphere is divided into layers of atmospheric thickness d_I . After the traversing of each layer the number of charged pions is assumed to be M_{ch} times larger if $d_I = \lambda_I \ln 2$, where $\lambda_I = 120 \text{ g cm}^{-2}$ is the interaction length of strongly interacting pions. Consequently, after n layers the number of charged pions is $(M_{\text{ch}})^n$. The energy per pion is

$$E_{\pi,n} = \frac{E_0}{M^n} . \quad (2)$$

The stopping energy is estimated on the basis of the finite lifetime of the pions in the atmosphere. For this it suffices to consider the approximate relation between atmospheric depth and height:

$$X(h) = 1030 \cdot e^{-h/8} \leftrightarrow h(X) = 8 \ln(1030/X) , \quad (3)$$

where X is the depth in g cm^{-2} and h is the height in km. Neutral pions decay almost immediately into two photons, $c\tau = 25 \text{ nm}$ [6]. Each resulting photon starts an electromagnetic shower. The decay length of the charged pions is $\gamma c\tau$, where $c\tau = 7.8 \text{ m}$ [6]. The decay length is of the order of a

kilometer because of the relativistic time dilation. As a consequence charged pions may interact with the atmosphere and propagate the hadronic shower, before decay. If the probability for decay in the next layer is larger than the probability of a hadronic interaction, the pions are assumed to decay and the cascade stops. This happens after n_c layers. The corresponding energy of the decaying charged pions, the stopping energy ξ_c^π , follows from

$$\xi_c^\pi = \frac{E_0}{M^{n_c}} . \quad (4)$$

The stopping energy turns out to be around 20 GeV.

2 Model parameters

In this paper the Heitler-Matthews model is extended to all the generations of pions in the shower. The complete analysis will be improved by consequently taking the multiplicity M and interaction length λ_I to depend on the energy of the hadron in the shower. One of the consequences is that the thickness of the cascade layers increases with depth, see Fig. 1.

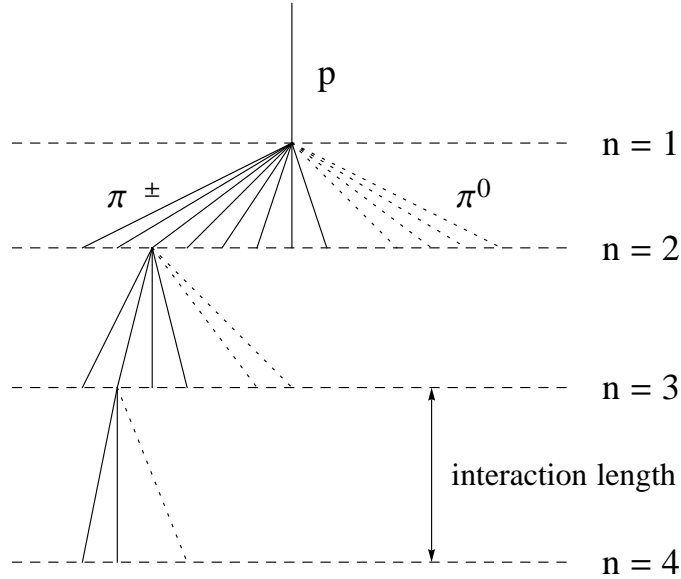


Figure 1: The hadronic cascade for energy dependent interaction lengths.

We will take the energy dependence of the π -air multiplicity and interaction length to be given by Monte Carlo event generators based on QCD and parton models. The calculated π -air charged multiplicity, see Fig. 5 of [7], Fig. 7 of [8] and Fig. 5 of [9], suggests the relation

$$M_{\text{ch}} \approx 0.1 \cdot E^{0.18} , \quad (5)$$

where E is the energy in eV. Taking the ratio of the charged and neutral pions as 2 : 1, we have for the total multiplicity

$$M \approx 0.15 \cdot E^{0.18} , \quad (6)$$

It should be emphasized that the relation between multiplicity and energy is rather uncertain since different models predict different multiplicities. In particular for large energies the differences can be large, even more than 100%. From Fig. 5 of [7] and Fig. 7 of [8] we see that the pion multiplicity does not differ substantially from the proton multiplicity. We therefore will use the relations (5) and (6) for both the multiplicity in proton-air (p-air) and pion-air (π -air) interactions. A parameterization with other values for the constants will, of course, affect the results quantitatively. It does, however, not alter the results qualitatively.

Both the p-air and π -air production cross sections grow with energy. The p-air production cross section at large energies obtained from observations of extensive air showers are in good agreement with QGSJET predictions [10, 11, 12, 13]. For the present analysis we will therefore use the QGSJET predictions for the p-air production cross section. We will also use the QGSJET predictions for the π -air production cross section [8, 14]. From these cross sections approximations for the energy dependent interaction lengths can be derived which are sufficiently accurate for our purpose. For π -air this is:

$$\lambda_{\pi\text{-air}} [\text{g cm}^{-2}] \approx 200 - 3.3 \ln(E[\text{eV}]) . \quad (7)$$

For p-air this is

$$\lambda_{\text{p-air}} [\text{g cm}^{-2}] \approx 145 - 2.3 \ln(E[\text{eV}]) . \quad (8)$$

Before we turn to the analysis we first consider general multiplicative growth processes for fixed interaction lengths and several fixed multiplicities.

3 Multiplication statistics

In this section we will revisit the relation $d_I = \lambda_I \ln 2$ as it is used in the Heitler-Matthews model for hadronic air showers [2, 3]. The latter might be motivated by the expression $\lambda_r \ln 2$ for the splitting length in the electromagnetic cascade. There the ratio $\ln 2$ results from the translation of the radiation length to the splitting length. In an intermediate model for electromagnetic showers the splitting length, $\lambda_r \ln 2$, is effectively used as the electromagnetic interaction length [15]. For the hadronic cascade, however, there is no a priori reason for the ratio $\ln 2$ between layer thickness and interaction length. Since λ_I is already an interaction length, the ratio between layer thickness and interaction length is rather expected to be 1.

For certainty we investigate the ratio by means of a pure mathematical multiplication model.

Assuming interactions occur randomly with an average atmospheric depth interval λ_I , the number of interactions in a layer of the atmosphere with a thickness X is Poisson distributed with the interaction length λ_I as the parameter:

$$P(k) = \frac{1}{k!} \left(\frac{X}{\lambda_I} \right)^k e^{-\frac{X}{\lambda_I}} . \quad (9)$$

If each interaction produces M_{ch} charged particles and if the number of interactions is unlimited, the expectation value of the number of charged particles at depth X would be

$$N = \sum_{k=0}^{\infty} \frac{1}{k!} \left(\frac{M_{\text{ch}} X}{\lambda_I} \right)^k e^{-\frac{X}{\lambda_I}} \equiv e^{\frac{X}{\lambda_I} (M_{\text{ch}} - 1)} . \quad (10)$$

Obviously, without a stopping criterion the number of particles grows exponentially. For a growth according to a Heitler model with a production of M_{ch} particles after each length d_I , the number of charged particles at depth X would be

$$N = M_{\text{ch}}^{X/d_I} , \quad X < n_c d_I . \quad (11)$$

The latter agrees with the result (10) if

$$d_I = \lambda_I \frac{\ln M_{\text{ch}}}{M_{\text{ch}} - 1} . \quad (12)$$

The latter expression is an asymptotic value corresponding to the situation where no stopping criterium is implemented. When the number of particles in the shower is large enough the probabilities of the Poisson distribution can be regarded as fractions of the shower. The expression (12) is valid for this situation. However, initially there is just a single cosmic ray particle. Since for a single particle the probabilities of the Poisson distribution can not be regarded as fractions of a shower the mean depth at which the primary particle interacts is λ_I and not the d_I as given by (12). After the first interaction there are already so many secondary particles that most of the probabilities will be realized leading to a production length close to the value given by (12). This is even more so after the second interaction. Without a stopping criterion the asymptotic value (12) would be reached in a few steps. In reality the stopping mechanism limits the number of interactions. As a consequence the growth is substantially reduced already after a few steps. This results in values for d_I larger than the limit value (12), after some more steps to even larger values than λ_I .

What we need for the present analysis is a mean value of d_I , averaged over

the cascade. To obtain this value we consider the limited growth model for several different multiplicities. For this purely mathematical investigation there is no need to distinguish between charged and full multiplicities. We will take a single mathematical multiplicity, conveniently denoted as μ . Also for convenience, we describe the situation with respect to a dimensionless depth t in units of interaction length: $t = X/\lambda_I$. The maximum number of interactions (until the charged pions decay) will be denoted as k_{\max} . Then the expectation value of the number of particles at depth t is

$$N = \sum_{k=0}^{k_{\max}} \frac{(\mu t)^k}{k!} e^{-t} . \quad (13)$$

The multiplicities we will consider are $\mu = 2, 3, 5$ and 10 . For each μ we take the value of k_{\max} such that $\mu^{k_{\max}} \approx 1.5 \cdot 10^6$. That is, $k_{\max} = 20, 13, 9$ and 6 respectively. If the stopping energy is about 20 GeV these figures correspond to primary energies of about 30 PeV. We mention the latter to give an idea, although it is the presence of a k_{\max} which is relevant and not the size of k_{\max} . On the basis of the truncated summation (13) the particle number N is plotted against t for $\mu = 2, 3, 5$ and 10 , see the dashed curves in the four separate diagrams of Fig. 2.

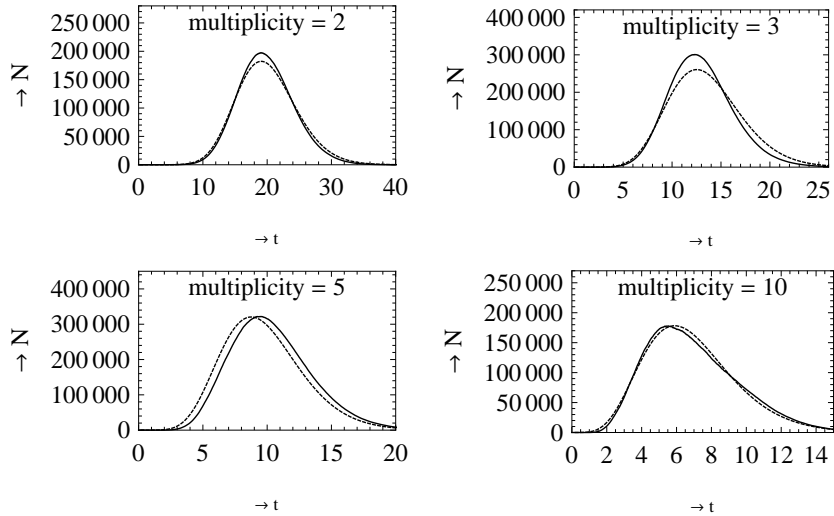


Figure 2: The number of particles against depth in units of interaction length for the following pairs of multiplicity and k_{\max} : (2,20) (upper left), (3,13) (upper right), (5,9) (lower left) and (10,6) (lower right), on the basis of the truncated series (13) (dashed) and on the basis of a full simulation where each individual particle is tracked (solid).

The first term in (13), e^{-t} , is the probability for a particle to survive a depth

t . On the basis of this probability also full Monte Carlo simulations are conducted of the survival lengths of each individual particle in a shower. The number of particles at a certain depth, obtained by binning, are shown as solid curves in Fig. 2.

Although the Monte Carlo simulation is more realistic, it has the disadvantage that every generated shower is a particular realization and not a statistical mean. Every simulation results in a slightly different curve. Therefore there is no sense in a precise comparison between the curves in Fig. 2. It does however show the general agreement between the shower development based on a Monte Carlo simulation and on the Poisson distribution. In both cases the depth of maximum shower size is about k_{\max} . To obtain a more precise analytical estimate of the depth of maximum shower size we will make use of the fact that the number of particles according to the truncated series (13) follows a similar curve as the number of particles corresponding to the last term of the series (13). A plot of the first differs from a plot of the latter just by a small shift δ towards a smaller depth and by a larger amplitude. Denoting the amplitude ratio as A , we have

$$\sum_{k=0}^{k_{\max}} \frac{(\mu t)^k}{\Gamma(k+1)} \approx \frac{A (\mu t)^{k_{\max}-\delta}}{\Gamma(k_{\max}+1-\delta)} , \quad (14)$$

where Γ is the Gamma function. Substitution in the identity

$$\sum_{k=0}^{k_{\max}+1} \frac{(\mu t)^k}{\Gamma(k+1)} = \frac{(\mu t)^{k_{\max}+1}}{\Gamma(k_{\max}+2)} + \sum_{k=0}^{k_{\max}} \frac{(\mu t)^k}{\Gamma(k+1)} \quad (15)$$

leads to the equation

$$\frac{A (\mu t)^{k_{\max}+1-\delta}}{\Gamma(k_{\max}+2-\delta)} \approx \frac{(\mu t)^{k_{\max}+1}}{\Gamma(k_{\max}+2)} + \frac{A (\mu t)^{k_{\max}-\delta}}{\Gamma(k_{\max}+1-\delta)} . \quad (16)$$

Evaluating at $t = k_{\max} + 1 - \delta$, we obtain

$$A \approx \frac{\mu^{1+\delta}}{\mu-1} \cdot \frac{\Gamma(k_{\max}+2-\delta)}{\Gamma(k_{\max}+2)} \cdot (k_{\max}+1-\delta)^\delta . \quad (17)$$

A series expansion for A approximately yields

$$A \approx \frac{\mu^{1+\delta}}{\mu-1} \cdot \left(1 - \frac{\delta(\delta+1)}{2k_{\max}} \right) . \quad (18)$$

By numerical inspection it is found that good fits are obtained for

$$\delta \approx \frac{1}{\mu-1} . \quad (19)$$

For the four pairs of values $(\mu, k_{\max}) = (2, 20)$, $(3, 13)$, $(5, 9)$ and $(10, 6)$ the number of particles is plotted according to the approximation

$$N \approx \frac{A(\mu t)^{k_{\max}-\delta}}{\Gamma(k_{\max} + 1 - \delta)} e^{-t}, \quad (20)$$

with δ as given by (19) and A as given by (18), see solid curves in Fig. 3. For comparison the number of particles is plotted according to the truncated summation (13) as well, see the dashed curves in Fig. 3.

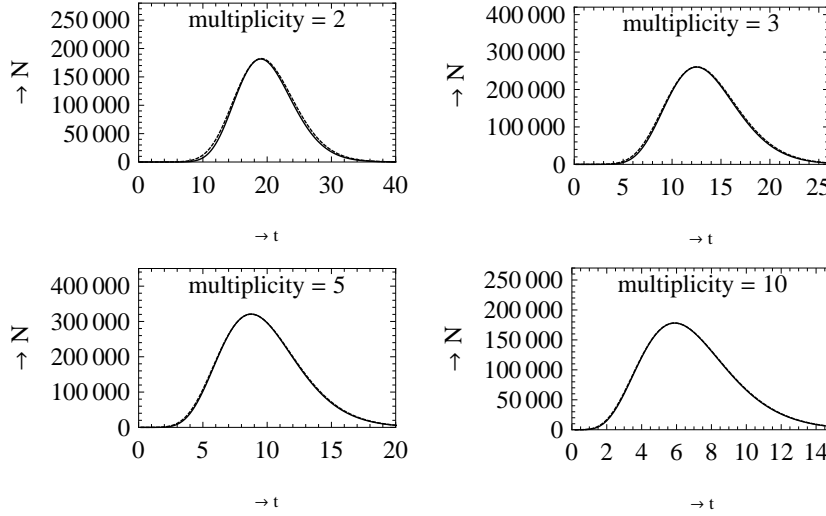


Figure 3: The number of particles against depth in units of interaction length for the following pairs of multiplicity and k_{\max} : $(2, 20)$ (upper left), $(3, 13)$ (upper right), $(5, 9)$ (lower left) and $(10, 6)$ (lower right), on the basis of the truncated series (13) (dashed) and on the basis of the approximation (20) (solid).

The two curves in each diagram of Fig. 3 are practically identical; they can hardly be distinguished. The agreement even increases with multiplicity. Therefore approximation (20) can be used for the analytic determination of the depth of maximum shower size. From the approximation (20) it follows that $N(t)$ reaches its maximum when $t = k_{\max} - \delta$. If we return to physics for a moment, in hadronic interactions the multiplicity is of order 10 and larger. The corresponding values for δ are smaller than 0.1 and can in practice be neglected: $t_{\max} \approx k_{\max}$.

The conclusion of the whole analysis is that the mean interaction length is $X_{\max}/k_{\max} = \lambda_I$. For this reason we take $d_I = \lambda_I$ as the characteristic length over which the number of particles is increased by a factor μ . For clarity, $d_I < \lambda_I$ in the initial stage of the shower when the shower number

is exponentially growing and $d_I > \lambda_I$ when the number of particles in the shower approaches its maximum. As a cascade average $d_I = \lambda_I$. We therefore will take $d_I = \lambda_I$ in the present model. In this respect we deviate from Matthews and Hörandel who take $d_I = \lambda_I \ln 2$ [2, 3].

4 The hadronic cascade for a primary proton

Now we consider a hadronic cascade where the hadronic particles interact after having traversed a layer of atmosphere. As argued in the previous section the thickness of each layer will be taken equal to the actual interaction length λ_I as given by (7) or (8). After each interaction M pions are produced as given by (6). In accordance with the Heitler model for electromagnetic showers, the energy is assumed to be equally divided over the particles produced. After each interaction the new energy of the charged hadrons then follows from a successive application of the equation

$$E_{j+1} = \frac{E_j}{M(E_j)} . \quad (21)$$

Starting with a primary proton with energy E_0 the energy of the particles after the first interaction is

$$E_1 = \frac{E_0}{0.15 \cdot E_0^{0.18}} \approx 6.7 \cdot E_0^{0.82} . \quad (22)$$

After the second interaction this is

$$E_2 = \frac{E_1}{0.15 \cdot E_1^{0.18}} \approx 6.7 \cdot E_1^{0.82} \approx 6.7^{1.82} \cdot E_0^{0.82^2} . \quad (23)$$

Repeating the iteration we find for the energy per particle after n interactions

$$E_n = 6.7^{\alpha_n} \cdot E_0^{\beta_n} , \quad (24)$$

where

$$\alpha_n = \frac{1 - 0.82^n}{1 - 0.82} , \quad \beta_n = 0.82^n . \quad (25)$$

For the interaction lengths we obtain for the primary proton, $n = 0$,

$$\lambda_0 = \lambda_{\text{p-air}}(E_0) = 145 - 2.3 \ln(E_0) \quad (26)$$

and for the produced pions, $n \geq 1$,

$$\lambda_n = \lambda_{\pi\text{-air}}(E_n) = 200 - 3.3 \ln(E_n) . \quad (27)$$

With the substitution of (24) this is

$$\lambda_n = 200 - 6.3\alpha_n - 3.3\beta_n \ln(E_0) , \quad n \geq 1 . \quad (28)$$

The atmospheric depth of the n_c -th interaction is given by

$$X(n_c) = \sum_{n=0}^{n_c-1} \lambda_n, \quad n_c \geq 1. \quad (29)$$

Substitution of (26) and (28) leads to

$$X(n_c) = 200n_c - 55 - 6.3 \sum_{n=1}^{n_c-1} \alpha_n - \left(2.3 + 3.3 \sum_{n=1}^{n_c-1} \beta_n \right) \ln(E_0). \quad (30)$$

With the approximate relation (3) between height and atmospheric depth, we obtain for the difference in height between the n_c -th and $(n_c + 1)$ -th interaction:

$$\Delta h[\text{km}] = 8 \ln \left(\frac{X(n_c + 1)}{X(n_c)} \right). \quad (31)$$

For the decay length of the charged pions after the n_c -th interaction we find

$$c\tau\gamma[\text{km}] \approx 7.8 \cdot 10^{-3} \frac{E_{n_c}}{m_{\pi\pm}} \approx 5.6 \cdot 10^{-11} \cdot 6.7^{\alpha_{n_c}} \cdot E_0^{\beta_{n_c}}, \quad (32)$$

where we have taken 140 MeV/c² for the mass of the charged pions [6]. We will follow Matthews with the reasonable assumption that the pions will decay when the decay length is half the layer thickness: $\gamma c\tau \approx \frac{1}{2} \Delta h$ [2]. That is

$$5.6 \cdot 10^{-11} \cdot 6.7^{\alpha_{n_c}} \cdot E_0^{\beta_{n_c}} = 4 \ln \left(\frac{X(n_c + 1)}{X(n_c)} \right), \quad (33)$$

In this equation we substitute integer values for n_c and solve numerically for the primary energy E_0 . Results of interest are shown in table 1, 2 and 3. In table 1 the height h is calculated with Eq. (3). In table 2 and 3 the interaction lengths respectively multiplicities are given for all interactions up to the final one after which decay occurs. Of course, the number of interactions in the cascade and thus also the penetration depth of the shower increases with the energy of the primary particle. Since a larger atmospheric depth at a lower altitudes corresponds to a larger probability for a charged pion to interact before decay, we expect a smaller stopping energy. From the last entry in table 1 we see the stopping energy indeed decreases for increasing primary energy.

The number of muons is given by

$$N_\mu = \left(\frac{2}{3} \right)^{n_c} \cdot \prod_{n=0}^{n_c-1} M_n. \quad (34)$$

For a primary proton with energy $1.4 \cdot 10^{15}$ eV, as an example, the number of muons is about $1.6 \cdot 10^4$. The energy of the final pions is about $2.6 \cdot 10^{10}$

n_c	E_0 [eV]	$X(n_c)$	$X(n_c + 1)$	$h(n_c)$ [km]	Δh [km]	ξ_c^π [eV]
1	$1.5 \cdot 10^{12}$	81	198	20.4	7.2	$6.4 \cdot 10^{10}$
2	$2.9 \cdot 10^{13}$	184	303	13.8	4.0	$3.6 \cdot 10^{10}$
3	$1.4 \cdot 10^{15}$	275	396	10.6	2.9	$2.6 \cdot 10^{10}$
4	$1.9 \cdot 10^{17}$	352	473	8.6	2.4	$2.1 \cdot 10^{10}$
5	$8.2 \cdot 10^{19}$	409	531	7.4	2.1	$1.9 \cdot 10^{10}$

Table 1: Characteristics of hadronic cascades for a primary proton.

n_c	E_0 [eV]	λ_0	λ_1	λ_2	λ_3	λ_4	$\bar{\lambda}$
1	$1.5 \cdot 10^{12}$	81	–	–	–	–	81
2	$2.9 \cdot 10^{13}$	74	110	–	–	–	92
3	$1.4 \cdot 10^{15}$	65	99	111	–	–	92
4	$1.9 \cdot 10^{17}$	53	86	100	112	–	88
5	$8.2 \cdot 10^{19}$	40	70	87	101	112	82

Table 2: Subsequent interaction lengths in hadronic cascades for a primary proton. The λ_n and the cascade average $\bar{\lambda}$ are in g cm^{-2} .

n_c	E_0 [eV]	M_0	M_1	M_2	M_3	M_4	\bar{M}
1	$1.5 \cdot 10^{12}$	23	–	–	–	–	23
2	$2.9 \cdot 10^{13}$	40	20	–	–	–	28
3	$1.4 \cdot 10^{15}$	80	36	19	–	–	38
4	$1.9 \cdot 10^{17}$	193	75	34	18	–	55
5	$8.2 \cdot 10^{19}$	576	183	72	33	18	85

Table 3: Subsequent multiplicities and their geometric mean in hadronic cascades for a primary proton.

eV, see last entry of table 1. For the quantity

$$\beta = \frac{\ln N_\mu}{\ln (E_0/\xi_c^\pi)} \quad (35)$$

we then obtain the value 0.89. For other primary energies the value of β is found to increase slightly from 0.88 through 0.92 for a primary energy increasing from 10^{12} eV through 10^{20} eV. Since we work with larger multiplicities, these values are slightly larger than the one obtained by Matthews [2].

From the last column in table 3 we find the following approximate relation between the effective multiplicity (the geometric mean multiplicity) and the primary energy: $\ln \bar{M} \approx 1.05 + 0.074 \ln E_0$. The effective charged multiplicity then is given by $\ln \bar{M}_{\text{ch}} \approx 0.65 + 0.074 \ln E_0$. Substituting the latter in the Matthews' expression [2]

$$\beta = 1 - \frac{\kappa}{3 \ln M_{\text{ch}}} \quad , \quad (36)$$

where κ is the inelasticity, we obtain a refinement for the energy dependence:

$$\beta = 1 - \frac{\kappa}{1.9 + 0.22 \ln E_0} \quad . \quad (37)$$

5 Hybrid Heitler scheme

The Heitler line of reasoning can also be applied to electromagnetic shower profiles other than the Heitler profile (1). Let $N(X; E)$ be an electromagnetic shower profile which for a primary energy E has its maximum $N_{\text{max}}(E)$ at depth $X_{\text{max}}(E)$. For twice the primary energy the particle will split into two particles with energy E after one splitting length $d = \lambda_r \ln 2$. The corresponding shower profile can be regarded as twice the shower profile for E shifted with d towards a larger depth. As a consequence $N_{\text{max}}(2E) = 2N_{\text{max}}(E)$ and $X_{\text{max}}(2E) = X_{\text{max}}(E) + d$. The elongation rate therefore is

$$\frac{dX_{\text{max}}}{d \ln E} = \lambda_r \quad . \quad (38)$$

This scheme will be applied to the present hadronic cascades. Each time when neutral pions decay into photons an electromagnetic subshower is initiated and the corresponding longitudinal profile is substituted. It is similar to what is done in the hybrid Monte Carlo model CONEX [16]. For the electromagnetic shower profile we take the Greisen function [17]:

$$N_e(X) = \frac{0.31}{\sqrt{y_c}} \cdot e^{\frac{X}{\lambda_r}(1-1.5 \ln s)} \quad , \quad (39)$$

where $y_c = \ln(E_0/\xi_c^e)$ and where

$$s = \frac{3X}{X + 2X_{\max}} \quad (40)$$

is the age parameter. For showers initiated by a photon a good prediction for the depth of maximum is given by

$$X_{\max,\gamma} [\text{g cm}^{-2}] = n_c \cdot d = y_c \cdot \lambda_r \approx 37 \ln E_0 - 675 \quad . \quad (41)$$

For energies larger than 1 EeV, the depth of maximum for photon showers is larger than predicted by (41) because of the Landau-Pomeranchuk-Migdal (LPM) effect [19, 20, 21]. See for instance the corresponding curve in Fig. 13 of [18]. By means of a hybrid Monte Carlo model the consequences of the LPM effect for hadronic air showers are found negligible for primary energies below $3 \cdot 10^{20}$ eV [8]. For such extremely high primary energies the large multiplicity causes the energy of the decay photons after the first interaction to be below 1 EeV, outside the LPM regime. We will therefore conveniently take (41) for the depth of maximum shower size of electromagnetic (sub)showers. The total electromagnetic shower profile is obtained by adding the profiles of the electromagnetic subshowers. An illustration is given in Fig. 4.

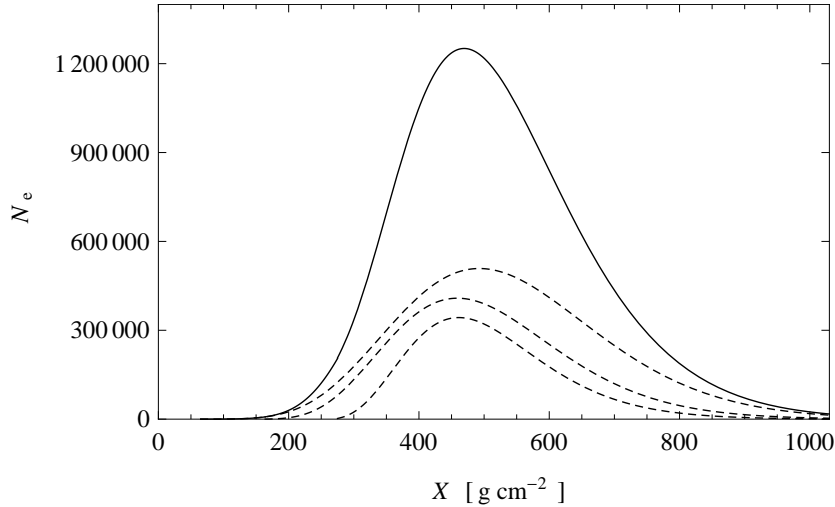


Figure 4: Total electromagnetic shower profile (solid) as it results from the addition of the profiles of the electromagnetic subshowers (dashed) for a 1.4 PeV proton primary.

The maximum number of electrons and positrons of the total electromagnetic shower is found by numerical inspection. This semi-analytical approach is utilized to be able to consider all the generations of subshowers. The number of muons is found by means of Eq. (34). In Fig. 5 we have plotted the

maximum size of the total electromagnetic shower and the number of muons as a function of initial energy.

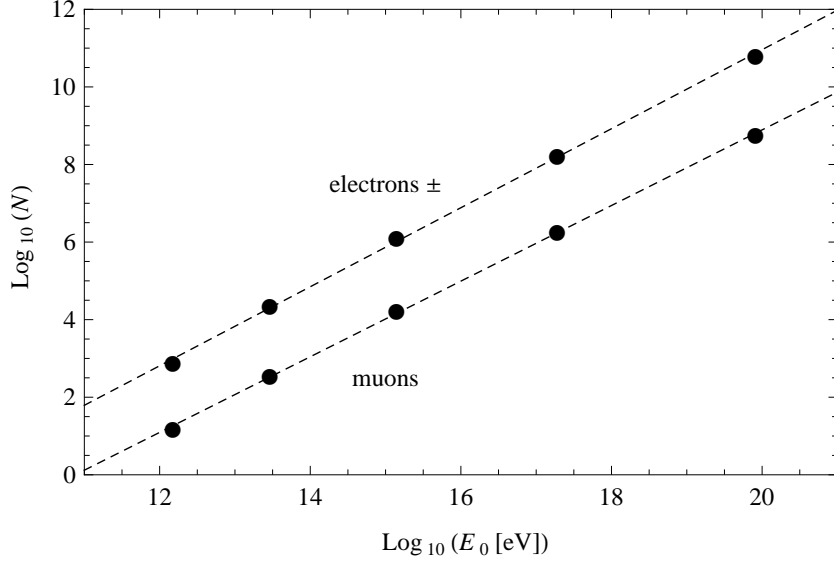


Figure 5: The maximum number of electrons (\pm) and muons as a function of the energy of the primary proton (dots) and the linear fits (dashed).

A linear fit, see the dashed lines in Fig. 5, for the maximum number of electrons (\pm) and number of muons yields

$$N_e \approx 0.57 \cdot (E_0[\text{GeV}])^{1.019} \quad (42)$$

and

$$N_\mu \approx 0.015 \cdot (E_0[\text{GeV}])^{0.975} \quad (43)$$

respectively. The values of $N_e + 25N_\mu$ for different values of the primary proton energy E_0 are close to the ones obtained with Monte Carlo models, e.g. Fig. 3 of [22].

The depth of the maximum shower size of the total electromagnetic shower is also determined by numerical inspection. In Fig. 6 the depth of maximum shower size is plotted as a function of the energy of the primary proton.

A cubic fit, see the dashed line in Fig. 6, yields

$$X_{\text{max},p} \approx -1796 + 136.5 \ln E_0 - 2.810(\ln E_0)^2 + 0.0217(\ln E_0)^3. \quad (44)$$

The latter expression is the result for a primary proton as indicated by the subscript p . It parametrizes the energy dependence of the elongation rate. However, the model itself is a simplification of reality and therefore not

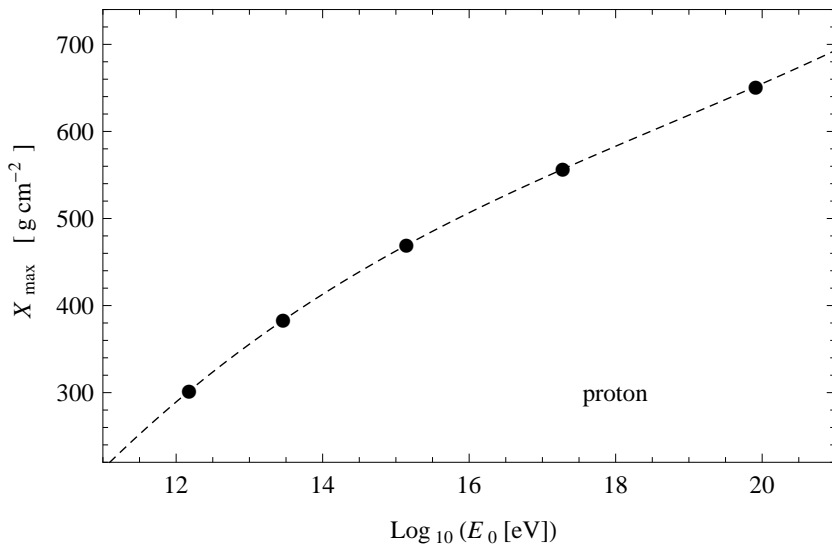


Figure 6: The depth of maximum shower size as a function of energy of a proton primary for the situation with complete inelasticity (dots) and the corresponding cubic fit (dashed).

accurate. Given all the caveats to obtain the present model, a linear fit may be more appropriate:

$$X_{\text{max,p}} \approx -223 + 19.4 \ln E_0 . \quad (45)$$

The latter expression corresponds to an energy independent elongation rate. It will be used for a comparison with Monte Carlo results in the final section. An analytical estimate can be obtained by considering solely the first generation of γ 's [2, 3]. Then, with the present model parameters,

$$X_{\text{max,p}} \approx \lambda_{\text{p-air}} + X_{\text{max},\gamma}(E_0/(2M)) \approx -485 + 28.0 \ln E_0 . \quad (46)$$

Clearly, the elongation rate in the latter expression is substantially larger than in Eq. (45). It is of application to small energies where there is a single generation of γ 's. For larger energies the elongation rate is overestimated by Eq. (46).

6 Iron primary

The hadronic cascade for an iron primary differs from the one for a proton primary by a smaller depth of first interaction and by a larger multiplicity in the first interaction. The iron-air cross section is about 2000 mb, see Fig. 54 of [23]. The corresponding interaction length is $\lambda_{\text{Fe-air}} \approx 12 \text{ g cm}^{-2}$. The

relatively small energy dependence of the iron-air cross section will only lead to a negligible difference of a few g cm^{-2} . According to the superposition model [17] the multiplicity of a composite nucleus with atomic mass A is equal to A times the multiplicity of a proton with a A times smaller energy:

$$M_{ch} = 0.1A \cdot \left(\frac{E_0}{A} \right)^{0.18} . \quad (47)$$

For iron-air, $A = 56$, this is $M_{ch} = 2.7 \cdot E_0^{0.18}$. Since not all nucleons will participate in the same rate as a single proton, the latter should be multiplied by a factor smaller than unity. If this factor is (almost) independent on energy, the superposition model predicts a constant rate between the iron-air and proton-air multiplicity. This is indeed what is seen from QCD based models and from a color glass condensate approach, see Fig. 5 of [7] and Fig. 7 of [24]. On the basis of Fig. 5 of [7] we take in our model the iron-air multiplicity as

$$M_{ch} = 0.3E_0^{0.18} , \quad M = 0.45E_0^{0.18} . \quad (48)$$

In the absence of elasticity the iron-air multiplicity is only present in the first interaction. Except for these two adaptations the analysis is identical to the one for a primary proton. Starting with a primary iron with energy E_0 the energy of the particles after the first interaction is

$$E_1 = \frac{E_0}{0.45 \cdot E_0^{0.18}} \approx 2.2 \cdot E_0^{0.82} . \quad (49)$$

Without elasticity the subsequent interactions are governed by the pion multiplicity:

$$E_2 = \frac{E_1}{0.15 \cdot E_1^{0.18}} \approx 6.7 \cdot E_1^{0.82} . \quad (50)$$

Repeating the iteration we find for the energy per particle after n interactions

$$E_n = 6.7^{\alpha_{n-1}} \cdot E_1^{\beta_{n-1}} , \quad (51)$$

where α_n and β_n are as defined in section 3. Substitution of (49) gives

$$E_n = 6.7^{\alpha_{n-1}} \cdot 2.2^{\beta_{n-1}} \cdot E_0^{\beta_n} , \quad (52)$$

For the interaction lengths we have for the primary iron, $n = 0$,

$$\lambda_0 = \lambda_{\text{Fe-air}}(E_0) = 12 . \quad (53)$$

The interaction lengths for the produced pions, $n \geq 1$, are as given before.

$$\lambda_n = \lambda_{\pi\text{-air}}(E_n) = 200 - 3.3 \ln(E_n) . \quad (54)$$

With the substitution of (52) this is

$$\lambda_n = 200 - 6.3\alpha_{n-1} - 2.6\beta_{n-1} - 3.3\beta_n \ln(E_0) , \quad n \geq 1 . \quad (55)$$

The atmospheric depth of the n_c -th interaction, $n_c \geq 1$, becomes

$$X(n_c) = 200n_c - 188 - 6.3 \sum_{n=1}^{n_c-1} \alpha_{n-1} - 2.6 \sum_{n=1}^{n_c-1} \beta_{n-1} - 3.3 \ln(E_0) \sum_{n=1}^{n_c-1} \beta_n. \quad (56)$$

For the decay length of the charged pions after the n_c -th interaction we now find

$$c\tau\gamma[\text{km}] \approx 5.6 \cdot 10^{-11} \cdot 6.7^{\alpha_{n_c-1}} \cdot 2.2^{\beta_{n_c-1}} \cdot E_0^{\beta_{n_c}}. \quad (57)$$

So, for the depth of the decay of the pions we obtain the following equation:

$$5.6 \cdot 10^{-11} \cdot 6.7^{\alpha_{n_c-1}} \cdot 2.2^{\beta_{n_c-1}} \cdot E_0^{\beta_{n_c}} = 4 \ln \left(\frac{X(n_c + 1)}{X(n_c)} \right). \quad (58)$$

As before, we substitute integer values for n_c and solve numerically for the primary energy E_0 . Results of interest are shown in table 4, 5 and 6, the equivalents of table 1, 2 and 3.

n_c	E_0 [eV]	$X(n_c)$	$X(n_c + 1)$	$h(n_c)$ [km]	Δh [km]	ξ_c^π [eV]
1	$1.9 \cdot 10^{13}$	12	127	35.6	18.9	$1.7 \cdot 10^{11}$
2	$1.8 \cdot 10^{14}$	121	239	17.2	5.5	$4.9 \cdot 10^{10}$
3	$7.7 \cdot 10^{15}$	221	341	12.3	3.5	$3.1 \cdot 10^{10}$
4	$9.4 \cdot 10^{17}$	309	430	9.6	2.6	$2.4 \cdot 10^{10}$
5	$3.8 \cdot 10^{20}$	380	502	8.0	2.2	$2.0 \cdot 10^{10}$

Table 4: Characteristics of hadronic cascades for a primary iron.

For the energy entries in table 4 the maximum number of electrons and muons for an iron initiated air shower is calculated in a similar way as for the proton initiated air showers. The resulting curves, see Fig. 7, are practically identical to the ones for a proton primary in Fig. 5. A linear fit, see the dashed lines in Fig. 7, for the maximum number of electrons (\pm) and number of muons yields

$$N_e \approx 0.59 \cdot (E_0[\text{GeV}])^{1.010} \quad (59)$$

and

$$N_\mu \approx 0.0055 \cdot (E_0[\text{GeV}])^{1.016} \quad (60)$$

respectively. As for proton primaries, the values of $N_e + 25N_\mu$ for different values of primary iron energy E_0 are close to the ones obtained with Monte

n_c	E_0 [eV]	λ_0	λ_1	λ_2	λ_3	λ_4	$\bar{\lambda}$
1	$1.9 \cdot 10^{13}$	12	–	–	–	–	12
2	$1.8 \cdot 10^{14}$	12	109	–	–	–	60
3	$7.7 \cdot 10^{15}$	12	98	110	–	–	74
4	$9.4 \cdot 10^{17}$	12	85	100	111	–	77
5	$3.8 \cdot 10^{20}$	12	69	86	101	112	76

Table 5: Subsequent interaction lengths in hadronic cascades for a primary iron. The λ_n and the cascade average $\bar{\lambda}$ are in g cm^{-2} .

n_c	E_0 [eV]	M_0	M_1	M_2	M_3	M_4	\bar{M}
1	$1.9 \cdot 10^{13}$	110	–	–	–	–	110
2	$1.8 \cdot 10^{14}$	165	22	–	–	–	60
3	$7.7 \cdot 10^{15}$	325	38	20	–	–	63
4	$9.4 \cdot 10^{17}$	773	78	36	19	–	80
5	$3.8 \cdot 10^{20}$	2274	189	73	34	18	114

Table 6: Subsequent multiplicities and their geometric mean in hadronic cascades for a primary proton.

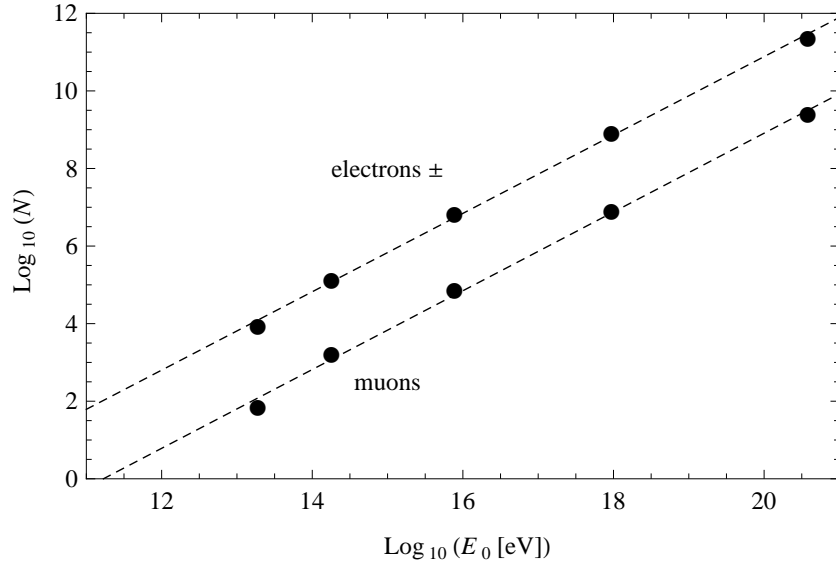


Figure 7: The maximum number of electrons (\pm) and muons as a function of the energy of the primary iron (dots) and the linear fits (dashed).

Carlo models, see Fig. 3 of [22].

Also the depth of maximum shower size for an iron primary is calculated in a similar way as for a proton primary. The result is shown in Fig. 8.

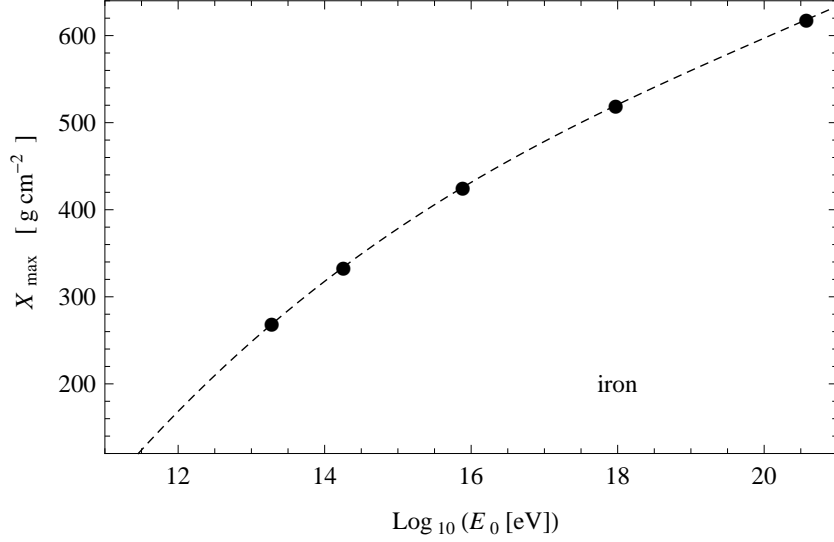


Figure 8: The depth of maximum shower size as a function of energy of an iron primary for the situation with complete inelasticity (dots) and the corresponding cubic fit (dashed).

Both the smaller interaction length and the larger multiplicity have reduced the depth of maximum shower size with respect to a proton initiated shower. A cubic fit, see the dashed line in Fig. 8, yields

$$X_{\max, \text{Fe}} \approx -2116 + 143.0 \ln E_0 - 2.721 (\ln E_0)^2 + 0.0194 (\ln E_0)^3, \quad (61)$$

where the subscript Fe identifies the primary particle. A linear fit yields

$$X_{\max, \text{Fe}} \approx -345 + 20.6 \ln E_0. \quad (62)$$

As for the proton a completely analytical estimate can be obtained by considering solely the first generation of γ 's:

$$X_{\max, \text{Fe}} \approx \lambda_{\text{Fe-air}} + X_{\max, \gamma}(E_0/(2M)) \approx -659 + 30.3 \ln E_0. \quad (63)$$

Also here the elongation rate in the analytical expression is substantially larger than in Eq. (62).

7 Conclusions and discussion

Hadronic cascades in cosmic air showers are analyzed by means of a Heitler-Matthews model extended to all generations of pions. For all the predictions a multiplicity and interaction length is applied parameterized for energy. It is argued that the thickness of the interaction layers should be taken equal to the interaction length and not a fraction $\ln 2$ of it. Although this increases the prediction for the depth of maximum shower size with a few tens of g cm^{-2} , the value for X_{max} still is too small in comparison with Monte Carlo results. It is also shown that an analysis based on the first generation of γ showers leads to an overestimation of the elongation rate. This implies that a better agreement with the Monte Carlo prediction for the elongation rate is accidental. Also the discrepancy between the depth of maximum shower size as predicted by the Heitler-Matthews model and as predicted by Monte Carlo models can not be explained by disregarding the second and further generations of γ 's. An alternative explanation is proposed below.

For a proton and iron primary the depth of maximum shower size as predicted by Monte Carlo models, see for instance the right panel of Fig. 10 of [9], Fig. 13 of [18] or Fig. 9 of [25], is about

$$X_{\text{max,p}} \approx -275 + 24 \ln E_0 \quad (64)$$

and

$$X_{\text{max,Fe}} \approx -585 + 29 \ln E_0. \quad (65)$$

respectively. These values are about 25% respectively 50% larger than as predicted by the present model:

$$-275 + 24 \ln E_0 \approx 1.25 \cdot (-223 + 19.4 \ln E_0) \quad (66)$$

respectively

$$-585 + 29 \ln E_0 \approx 1.5 \cdot (-345 + 20.6 \ln E_0) . \quad (67)$$

In the Heitler-Matthews model the energy of the interaction is assumed to be equally divided over the secondary particles. In reality the distribution of energy is highly inhomogeneous. This is observed in proton-proton collisions, see Fig. 48 of [26]. For proton-air collisions it is predicted by Monte Carlo models, see Fig. 6 of [18]. Many secondaries obtain a small part of the energy while a few particles obtain a larger part. The elasticity effect, where a substantial part of the energy is taken by the leading particle, can be regarded as the most profound manifestation of the inhomogeneous energy distribution. Both the elasticity and the inhomogeneous energy distribution over the non-leading secondaries increase the depth of maximum shower size. In our opinion the equal division of energy is therefore responsible for the

discrepancy with respect to shower simulators which have the inhomogeneous energy distribution incorporated. To give some foundation to the idea we consider the following relation [27]:

$$\frac{\Delta X_{\max}}{X_{\max}} \approx -\frac{1}{2} \frac{\Delta M}{M} - \frac{1}{10} \frac{\Delta \kappa}{\kappa} . \quad (68)$$

In this relation ΔX_{\max} is the shift of the depth of maximum shower size, M is the multiplicity and κ is the inelasticity. For protons and pions the inelasticity is roughly about $\frac{2}{3}$, see figure 6 of [8]. Starting from the inelastic situation, $\kappa = 1$, the change in inelasticity is $\Delta \kappa = -\frac{1}{3}$. According to the second part in the right hand side of Eq. (68) this corresponds to a shift

$$\Delta X_{\max} \approx \frac{1}{30} \cdot X_{\max} . \quad (69)$$

That is, about one seventh of the discrepancy can be explained by elasticity.

Also the the inhomogeneous energy distribution over the non-leading secondaries increase the depth of maximum shower size. Among the secondary charged pions there will be a few with relatively large energy who penetrate deeper into the atmosphere thereby contributing to the depth of maximum shower size in a similar way as elasticity does. At the same time there will be many secondary charged pions with energies so low that they will decay before they reach final generation of the cascade. In effect this reduces the cascade mean multiplicity. From the first part of the right hand side of Eq. (68) it follows that a substantial contribution to the shift ΔX can be expected. Since the effective reduction of multiplicity will be larger for large multiplicities and thus for large energies, the relative shift will be larger for large energies. As a consequence the inhomogeneous energy distribution over the non-leading secondaries does increase the depth of maximum shower size as well as the elongation rate. Since the multiplicity for iron is larger than for proton primaries, the larger discrepancy for iron primaries supports the idea that the discrepancy is related to the effective multiplicity and thus to the inhomogeneous energy distribution.

Of course, there also is the possibility of other contributions to the discrepancy. For instance, a part of the discrepancy might be an artefact of the discreteness of the hadronic cascade in the present model. We therefore can not say whether the inhomogeneous energy distribution over the non-leading secondaries explains all of the remaining part of the discrepancy. It seems however reasonable to expect that the inhomogeneous energy distribution is responsible for a large part of the difference between the depth of maximum shower size as predicted by Monte Carlo models and as predicted by the present model.

Acknowledgements

I wish to thank Dr. J.J.M. Steijger for his detailed and useful comments on an earlier draft of this paper. I wish to thank prof. J.W. van Holten and Prof. B. van Eijk for their useful comments and encouragement. I wish to thank Nikhef for its hospitality. The work is supported by a grant from NWO (Netherlands Organisation for Scientific Research).

References

- [1] W. Heitler, The Quantum Theory of Radiation, third ed., Oxford University Press, London, p. 386 (1954).
- [2] J. Matthews, Astropart. Phys. **22**, 387 (2005).
- [3] J. R. Hörandel, Mod. Phys. Lett. A, **22**, 1533 (2007).
- [4] R. Ulrich, R. Engel and M. Unger, Phys. Rev. D **83**, 054026 (2011).
- [5] R. engel, D. Heck and T. Pierog, Annu. Rev. Nucl. Part. Sci. **61**, 467 (2011).
- [6] Particle Data Group, Review of particle Physics, J. Phys. G **37**, 31 (2010).
- [7] S. Roesler, R. Engel and J. Ranft, SLAC-PUB-11093, 27th ICRC, Hamburg (2001).
- [8] J. Alvarez-Muñiz et al., Phys. Rev. D **66**, 033011 (2002).
- [9] J. Knapp et al., Astropart. Phys. **19**, 77 (2003).
- [10] R. Ulrich et al., New J. Phys. **11**, 065018 (2009).
- [11] P. Abreu et al, arXiv:1208.1520.v2 (2012).
- [12] M. Aglietta et al., EAS-TOP Collaboration, Phys. Rev. D **79**, 032004 (2009).
- [13] G. Aielli et al, ARGO Collaboration, Phys. Rev. D **80**, 092004 (2009).
- [14] T. Stanev, High Energy Cosmic Rays, 2nd ed., Springer-Verlag Berlin Heidelberg New York, 213 (2003).
- [15] J.M.C. Montanus, Astropart. Phys. **35**, 609 (2012).
- [16] T. Bergmann et al., Astropart. Phys. **26**, 420 (2007).
- [17] T. Gaisser, Cosmic Rays and Particle Physics, Cambridge University Press, Cambridge, p. 224 (1990).
- [18] H. Rebel and O. Sima, Rom. Journ. Phys. **57**, 472, (2012).
- [19] L. D. Landau and I. J. Pomeranchuk, Dokl. Akad. Nauk SSSR **92**, 535, (1953).

- [20] L. D. Landau and I. J. Pomeranchuk, Dokl. Akad. Nauk SSSR **92**, 735, (1953).
- [21] A. B. Migdal, Phys. Rev. **103**, 1811, (1956).
- [22] M.A.K. Glasmacher, Astropart. Phys. **12**, 1 (1999).
- [23] J. Knapp, D. Heck and G. Schatz, Forschungszentrum Karlsruhe Report **FZKA 5828**, (1996).
- [24] HJ. Drescher, arXiv:astro-ph/0612218v1, (2006).
- [25] J. R. Hörandel, J. Phys. G: Nucl. Part. Phys., **29**, 2439 (2003).
- [26] C. Alt et al., Eur. Phys. J. **45**, 343, (2006).
- [27] C. Pajares, D. Sousa and R.A. Vázquez, Astropart. Phys. **12**, 291, (2000).